IOPscience iopscience.iop.org

Home Search Collections Journals About Contact us My IOPscience

Optimal antibunching in passive photonic devices based on coupled nonlinear resonators

This article has been downloaded from IOPscience. Please scroll down to see the full text article.

2013 New J. Phys. 15 025012

(http://iopscience.iop.org/1367-2630/15/2/025012)

View the table of contents for this issue, or go to the journal homepage for more

Download details:
IP Address: 193.204.40.97
The article was downloaded on 08/02/2013 at 07:34

Please note that terms and conditions apply.

New Journal of Physics
The open access journal for physics

Optimal antibunching in passive photonic devices based on coupled nonlinear resonators

S Ferretti[1], **V Savona**[2] **and D Gerace**[1,3]

[1] Dipartimento di Fisica, Università degli Studi di Pavia, via Bassi 6, I-27100 Pavia, Italy
[2] Institute of Theoretical Physics, Ecole Polytechnique Fédérale de Lausanne (EPFL), CH-1015 Lausanne, Switzerland
E-mail: dario.gerace@unipv.it

New Journal of Physics **15** (2013) 025012 (13pp)
Received 10 October 2012
Published 7 February 2013
Online at http://www.njp.org/
doi:10.1088/1367-2630/15/2/025012

Abstract. We propose the use of weakly nonlinear passive materials for prospective applications in integrated quantum photonics. It is shown that strong enhancement of native optical nonlinearities by electromagnetic field confinement in photonic crystal resonators can lead to single-photon generation only exploiting the quantum interference of two coupled modes and the effect of photon blockade under resonant coherent driving. For realistic system parameters in state of the art microcavities, the efficiency of such a single-photon source is theoretically characterized by means of the second-order correlation function at zero-time delay as the main figure of merit, where major sources of loss and decoherence are taken into account within a standard master equation treatment. These results could stimulate the realization of integrated quantum photonic devices based on non-resonant material media, fully integrable with current semiconductor technology and matching the relevant telecom band operational wavelengths, as an alternative to single-photon nonlinear devices based on cavity quantum electrodynamics with artificial atoms or single atomic-like emitters.

[3] Author to whom any correspondence should be addressed.

Content from this work may be used under the terms of the Creative Commons Attribution-NonCommercial-ShareAlike 3.0 licence. Any further distribution of this work must maintain attribution to the author(s) and the title of the work, journal citation and DOI.

© IOP Publishing Ltd and Deutsche Physikalische Gesellschaft

Contents

1. Introduction

Emerging quantum photonic technologies mostly rely on the ability to generate, manipulate and detect quantum states of light, with the challenging goal of bringing quantum information and communication devices to large-scale applications (see [1, 2] for recent overviews). Single-photon sources (SPS) and linear optical operations are necessary ingredients for prospective developments in quantum information processing [3, 4], and remarkable progress toward a fully integrated and complementary metal-oxide-semiconductor (CMOS)-compatible technology has been achieved over the last few years [5]. However, the ability to generate pure single-photon Fock states on demand in a fully integrated quantum photonic platform is still lacking. Commonly employed SPS in quantum optical experiments rely on attenuated laser beams and parametric down-conversion. Typically, a coherent source of radiation is sent through a nonlinear medium possessing an intrinsic $\chi^{(2)}$ nonlinear susceptibility [6], which is able to produce entangled photon pairs and hence heralded single-photon states upon projective measurement of one of the two channels [7]. Even though such sources inevitably suffer from low efficiencies [8], this is currently the preferred way to inject single-photon wave packets as the input for integrated quantum circuits through external fiber coupling [5], although an integrated source of heralded single photons has recently been realized [9].

Generation of pure single-photon states requires a quantum nonlinear source, i.e. ideally a two-level emitter that is prepared in its excited state and produces exactly a single quantum of light per pulse when relaxing to its ground state. One of the measures of SPS efficiency is determined by the degree of antibunching in its second-order correlation function at zero-time delay, $g^{(2)}(0) < g^{(2)}(\tau)$, whereby an ideal SPS satisfies $g^{(2)}(0) \to 0$ [10]. Tremendous progress in solid-state SPS has been made since the development of artificial quantum emitters, such as semiconductor quantum dots or atomic-like defects in solids (for a review, see [8] and references therein). In practice, cavity quantum electrodynamics (CQED) is the most straightforward way of obtaining single-photon nonlinear behavior and hence an SPS on demand [11], allowing one to efficiently access the underlying anharmonicity introduced by a single atomic-like emitter through a high-finesse resonator [12, 13]. In solid-state CQED, the most promising results on single-photon emission have been originally achieved with III–V materials, by using non-resonantly excited semiconductor quantum dots coupled to photonic microcavity modes, either in the Purcell regime [14–16], in strong light–matter coupling [17, 18], or even through a direct coupling to a one-dimensional mode such as a nanowire [19] or a photon crystal

waveguide [20–22]. Single-photon nonlinear behavior in the strong light–matter coupling regime has been shown also under resonant excitation [23, 24], i.e. exploiting the photon blockade effect [25]. The latter occurs in systems where two photons inside a resonant cavity produce an anharmonic shift of its response frequency that is greater than the line broadening induced by losses and decoherence. Under such conditions, the transmission of a coherent light field is inhibited by the presence of a single photon within the cavity, until such a single-photon state is released: the system converts a low-power coherent state into single-photon streams at the same resonant frequency, thus behaving as a single-photon source. The efficiency of such a source can be assessed by measuring the antibunched $g^{(2)}(0)$ in the transmitting channel, as experimentally shown for the first time with single caesium atoms strongly coupled to an optical Fabry–Pérot cavity [26].

A similar device can be realized when using a Kerr-type nonlinear medium, which gives rise to an equivalent response in terms of the degree of photon antibunching of the transmitted field [27]. Theoretical proposals have been presented over the last few years to achieve single-photon blockade in solid-state systems with *resonant* Kerr-type nonlinearities, such as fully confined polariton boxes below the diffraction limit [28–33]. In the latter, the Coulomb interaction of electron–hole pairs in a semiconductor or insulating resonant medium is responsible for a Kerr-type nonlinear coefficient, potentially able to produce photon blockade. Owing to experimental difficulties in reaching diffraction-limited polariton confinement with a sufficiently large cavity lifetime, no evidence of quantum nonlinear behavior from these systems has been reported yet. Besides applications of such devices as SPS in integrated quantum photonics, technologies might be limited in the long term by a lack of suitable active media in the telecom band, necessary to be interfaced with long-distance communication networks, and the commonly cryogenic working temperatures [8].

The possibility to engineer an SPS based on single-photon blockade from *non-resonant* Kerr-type nonlinearities in passive devices (such as nano-structured silicon or GaAs platforms in the near infrared) could represent a breakthrough from quantum photonics perspectives. Firstly, it would allow large flexibility on the operational wavelengths to be engineered in the telecom band by the photonic confinement in the materials transparency window. Secondly, it would potentially allow room temperature operations and possibly the elevated temperatures required for telecom devices. Finally, it would only require a coherent pump source such as a standard fiber-coupled telecom laser, thus providing a compact, stable and relatively low-cost device. It is a common perception that ordinary nonlinear media are intrinsically unable to display significant single-photon nonlinear behavior and a very large number of photons are necessary for producing appreciable effects, owing to the small value of the $\chi^{(3)}$ elements in ordinary bulk media [34]. However, interesting perspectives might come from a proper nano-structuring of passive nonlinear materials, which could lead to strongly enhanced effective nonlinearities down to the single-photon level [35], especially using photonic crystal type confinement allowing one to reach ultra-high quality factors [36] and ultra-small confinement volumes [37] in a purely dielectric structure. Even though potentially not unrealistic, such a goal is still quite challenging with single resonators.

In this paper, we report on an alternative strategy to realize an integrated SPS based on non-resonant Kerr-type nonlinearity, which exploits the effects of quantum interference in coupled photonic resonators [32, 33]. These effects have been shown to arise even for a weak nonlinear response, namely for an anharmonic shift of the two-photon energy levels much smaller than the cavity mode linewidth. Although very small, this anharmonic shift is enough to introduce a

phase shift between different excitation pathways to the two-photon state, which for well chosen values of the system parameters suppresses its occupation as a result of destructive interference, leading to antibunching of the output light. We note that an analogous mechanism has already been characterized in the simplest CQED system—a two-level atom coupled to a single-mode resonator—in a seminal work by Carmichael [38]. For a given value of the anharmonic shift, this scheme is able to relax by more than three orders of magnitude the cavity loss rate over conventional photon blockade devices, making the mechanism perfectly viable, for example, with commonly achievable defect cavities in photonic crystal structures. For such structures, we further show that the photon antibunching is robust to typically expected rates of pure dephasing. A generalization of this scheme to multi-cavity arrays might give rise to interesting perspectives on the generation of continuous variable entangled states on chip [39]. In this work, we focus our analysis on the optimization of $g^{(2)}(0)$ as a figure of merit for SPS, leaving the specific characterization of the device output in terms of single-photon wave packets for future work. With this, we also expect this proposal to stimulate new research efforts in silicon quantum photonics and CMOS-compatible quantum information technology.

The paper is organized as follows. In section 2, we present the basic model, based on a master equation for the system Hamiltonian and dissipative terms including the effects of losses and dephasing. In section 3, we give an overview of the steady-state results, quantifying the optimized antibunching as a function of the system parameters, and test its robustness with respect to pure dephasing mechanisms. Finally, we draw conclusions from this work in section 4.

2. The model of driven/dissipative coupled nonlinear resonators

The formalism introduced in the previous work for a single resonator [35] can be straightforwardly generalized to the case of two tunnel-coupled resonators made of a Kerr-type nonlinear material, or a *photonic molecule*, schematically represented in figure 1. Each resonator is assumed to be single-mode, where $\hat{a}_i$ ($\hat{a}_i^\dagger$) define the destruction (creation) operator of a single photon ($i = 1, 2$ labels the two resonators). As in [32, 33], we consider the nonlinear second-quantized Hamiltonian

$$\hat{H} = \sum_{i=1,2} [\hbar\omega_i \hat{a}_i^\dagger \hat{a}_i + U_{\rm nl} \hat{a}_i^\dagger \hat{a}_i^\dagger \hat{a}_i \hat{a}_i] + J(\hat{a}_1^\dagger \hat{a}_2 + \hat{a}_2^\dagger \hat{a}_1) + F\, \mathrm{e}^{-\mathrm{i}\omega_L t} \hat{a}_1^\dagger + F^*\, \mathrm{e}^{\mathrm{i}\omega_L t} \hat{a}_1, \tag{1}$$

where the linear part describes two harmonic oscillators, neglecting the zero point energy, $J/\hbar$ is the tunnel coupling rate between the two resonators[4], and $F/\hbar$ is the coherent pump rate at the continuous wave laser frequency $\omega_{\rm L}$. Following the scheme introduced in [32], only one of the two resonators is driven, and light will be assumed to be collected only from the same. For the case of a passive nonlinear resonator, the nonlinear energy shift for each mode can be approximated as [35, 40]

$$U_{\rm nl} \simeq \frac{3(\hbar\omega_0)^2}{4\varepsilon_0} \frac{\overline{\chi}^{(3)}}{\overline{\varepsilon}_{\rm r}^2} \int |\vec{\alpha}_i(\mathbf{r})|^4 \, \mathrm{d}\mathbf{r} = \frac{3(\hbar\omega_0)^2}{4\varepsilon_0 V_{\rm eff}} \frac{\overline{\chi}^{(3)}}{\overline{\varepsilon}_{\rm r}^2}, \tag{2}$$

[4] We are assuming here that a tight-binding scheme for neighboring photonic resonators holds, in which the tunnel coupling rate derives from the overlap between the evanescent tails of the cavity mode profiles. Such a formal expression of the coupled modes is valid only in the perfectly resonant condition, i.e. $\omega_1 = \omega_2$, as we will assume in the following.

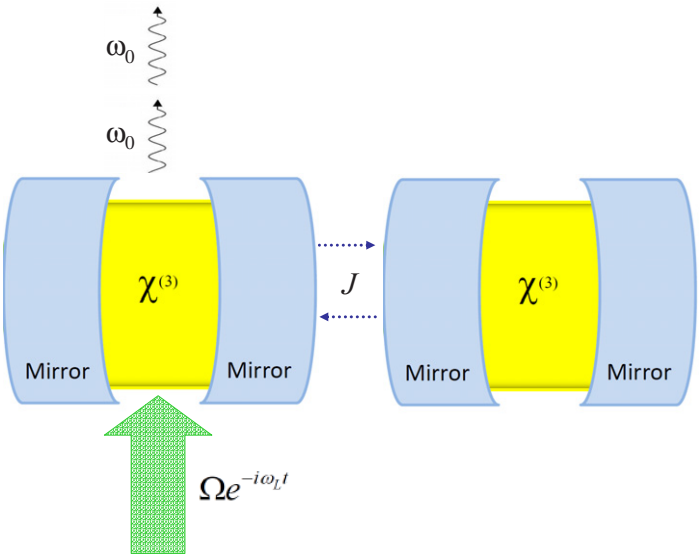

Figure 1. Scheme of two coupled resonators made of a Kerr-type nonlinear material. We highlight that just one of the cavities is resonantly driven by a coherent light source, and output light is collected from the same according to the scheme proposed in [32].

where the effective mode volume is defined as $V_{i,\mathrm{eff}}^{-1} = V_{\mathrm{eff}}^{-1} = \int |\vec{\alpha}_i(\mathbf{r})|^4 \, \mathrm{d}\mathbf{r}$, from the normalized field profile in each cavity, $\vec{\alpha}_i$, for the specific nanocavity implementation (see [41] for a review). For this purpose, we will assume constant values for the average real part of the nonlinear susceptibility and relative dielectric permittivity, $\overline{\chi}^{(3)}$ and $\overline{\varepsilon}_{\mathrm{r}}$, respectively, to have realistic order of magnitude estimates on materials of current technological interest[5]. The Hamiltonian can be expressed in a rotating frame with respect to the pump frequency, $\Delta\omega_i = \omega_i - \omega_{\mathrm{L}}$,

$$\hat{H} = \sum_{i=1,2} [\hbar \Delta\omega_i \hat{a}_i^\dagger \hat{a}_i + U_{\mathrm{nl}} \hat{a}_i^\dagger \hat{a}_i^\dagger \hat{a}_i \hat{a}_i] + J(\hat{a}_1^\dagger \hat{a}_2 + \hat{a}_2^\dagger \hat{a}_1) + F\hat{a}_1^\dagger + F^* \hat{a}_1. \tag{3}$$

The driven/dissipative character of this model is taken into account by a master equation treatment for the system density matrix in the Markov approximation

$$\dot{\rho} = \frac{1}{\mathrm{i}\hbar}[\rho, \hat{H}] + \mathcal{L}^{(1,2)} + \mathcal{L}^{\mathrm{deph}}, \tag{4}$$

where

$$\mathcal{L}^{(1,2)} = \sum_{i=1,2} \frac{\gamma_i}{2} [2\hat{a}_i \rho \hat{a}_i^\dagger - \hat{a}_i^\dagger \hat{a}_i \rho - \rho \hat{a}_i^\dagger \hat{a}_i] \tag{5}$$

is the Liouvillian operator in the usual Lindblad form for the two resonators modes, and

$$\mathcal{L}^{\mathrm{deph}} = \sum_{i=1,2} \frac{\gamma_i^*}{2} [2\hat{a}_i^\dagger \hat{a}_i \rho \hat{a}_i^\dagger \hat{a}_i - \hat{a}_i^\dagger \hat{a}_i \hat{a}_i^\dagger \hat{a}_i \rho - \rho \hat{a}_i^\dagger \hat{a}_i \hat{a}_i^\dagger \hat{a}_i] \tag{6}$$

models the pure dephasing for the two resonators modes.

[5] Note that we are neglecting self-consistent nonlinear effects on the cavity field profile induced by the Kerr nonlinearity itself (e.g. field expulsion from the cavity region), which could renormalize the effective value of U_{nl}.

In this work, we generalize the model to account for possible unbalanced losses between the two normal modes of the system. In the following, we will only consider the case $\Delta\omega_1 = \Delta\omega_2$ (with straightforward generalization), under which conditions one has the two symmetric and antisymmetric combinations, respectively, given by

$$\hat{a}_+ = \frac{1}{\sqrt{2}}(\hat{a}_1 + \hat{a}_2), \quad \hat{a}_- = \frac{1}{\sqrt{2}}(\hat{a}_1 - \hat{a}_2). \tag{7}$$

In this case, the losses can be described through the corresponding Liouvillian for the two coupled modes in the Lindblad form

$$\mathcal{L}^{(\pm)} = \frac{\gamma_+}{2}\left[2\hat{a}_+\rho\hat{a}_+^\dagger - \hat{a}_+^\dagger\hat{a}_+\rho - \rho\hat{a}_+^\dagger\hat{a}_+\right] + \frac{\gamma_-}{2}\left[2\hat{a}_-\rho\hat{a}_-^\dagger - \hat{a}_-^\dagger\hat{a}_-\rho - \rho\hat{a}_-^\dagger\hat{a}_-\right]. \tag{8}$$

One can easily show that when $\gamma_1 = \gamma_2 = \gamma$ and hence $\gamma_\pm = \gamma$, we obtain $\mathcal{L}^{(\pm)} = \mathcal{L}^{(1,2)}$, as expected. For the latter model, pure dephasing is taken into account by the Lindblad term as in equation (6), but for the operators $\hat{a}_+$ and $\hat{a}_-$.

3. Toward passive single-photon sources

We hereby analyze the device represented in the scheme of figure 1 as a potential SPS: a photonic molecule is driven by a low power input laser impinging only on cavity 1, and output light is collected from the same cavity (see the next section for a possible realization). The device could realize an efficient SPS if the light emitted from cavity 1 is strongly antibunched [32]. In the following, we assume the normalized degree of second-order coherence from the first resonator, $g^{(2)}(0) = \langle\hat{a}_1^{\dagger 2}\hat{a}_1^2\rangle/\langle\hat{a}_1^\dagger\hat{a}_1\rangle^2$, as the figure of merit quantifying the device efficiency.

3.1. Model parameters

We consider passive materials where the non-resonant nonlinearity is determined by the bulk contribution to the third-order material susceptibility, where the real part of the $\chi^{(3)}$ elements is responsible for the nonlinear frequency shift while the imaginary part gives rise to an additional contribution to losses, such as two-photon absorption (TPA). As shown in [35], TPA is essentially negligible for the low power intensities that would be required for single-photon nonlinear operation in such devices. For this reason, we will neglect its effect here. Typical semiconductor or insulator materials employed in the optoelectronic industry possess a real part of third-order susceptibility of the order of 10^{-19}–10^{-18} in Si units ($\mathrm{m^2\,V^{-2}}$) [34, 35]. We focus here on photonic crystal type confinement, where remarkable figures of merit (such as, e.g., ultra-high quality factors) have already been shown with both silicon (for a review, see [42]) and GaAs materials [43]. Moreover, a strong enhancement of second- and third-order nonlinearities has also been reported [43–45]. In such nanostructures, a realistic cavity mode confinement can be of the order of $V_{\mathrm{eff}} = (\lambda/n_{\mathrm{r}})^3 \simeq 0.1\,\mu\mathrm{m}^3$ (for near infrared operation, i.e. $\lambda \sim 1\,\mu$m and $n_{\mathrm{r}} = 3$ for typical semiconductors in this wavelength range), from equation (2) we have an estimate for the single-photon nonlinearity of the order of $U_{\mathrm{nl}} \simeq 10^{-3}\,\mu$eV. This is certainly a very small value, as compared to typical resonant nonlinearities induced by QD or QW transitions [28]. However, we aim at exploiting the photon blockade mechanism in weakly nonlinear tunnel-coupled devices, as introduced in [32]. To this end, we assume a very specific realization of such a proposal involving coupled photonic crystal cavities and access waveguides integrated on the same photonic chip, as schematically represented in figure 2. In

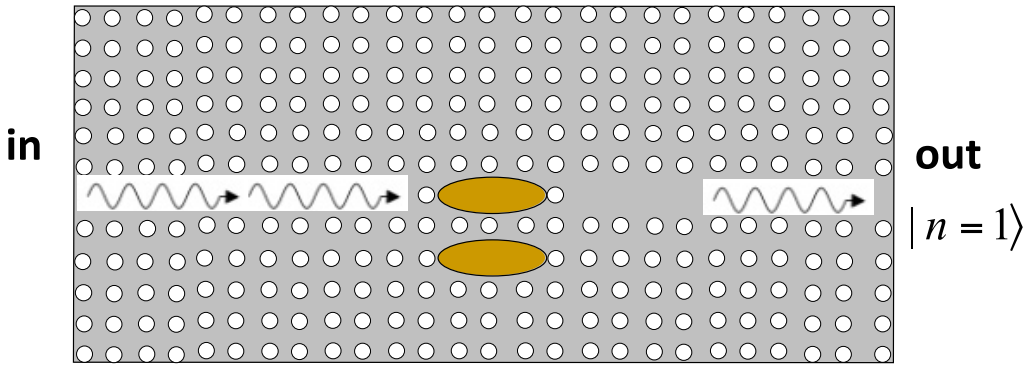

Figure 2. Sketch of a possible realization of an SPS based on the scheme shown in figure 1, with a photonic crystal integrated circuit fabricated with a nonlinear material as the underlying platform.

this case, typical tunnel-coupled micro-cavities display modes with spectral splitting of the order of $\Delta E_{\pm} = 2J \sim 1$ to a few meV [46, 47]. Finally, the quality factor of cavity modes in the near infrared is typically of the order of $Q \sim 10^4$–10^5, and we can safely assume $Q \sim 30\,000$ as a realistic value, which gives a typical cavity mode linewidth $\hbar\gamma \simeq 0.025$ meV for a resonance around $\hbar\omega_1 \simeq 0.8$ eV (the typical telecom wavelength $\lambda = 1.55\,\mu$m). Such realistic values for silicon- or GaAs-based photonic crystal chips at operational wavelengths in the most interesting telecom band allow us to assume normalized parameters in the model Hamiltonian (3) that are consistent with state-of-the-art semiconductor-based photonic technology: $U_{\rm nl} \sim 5 \times 10^{-5}$, $J \sim 50$ (in units of $\hbar\gamma$).

3.2. Optimal antibunching

Given the basic numbers, we now explore the efficiency of such SPS spanning the parameters space for the corresponding master equation, which is solved in its steady state by numerically determining a quantum average on $\rho_{\rm ss}$, which is the density matrix corresponding to the eigenvalue $\lambda_{\rm ss} = 0$ in the linear eigenvalue problem $\mathcal{L}\rho = \lambda\rho$.

First, in order to numerically infer the optimal resonance-pump detunings, we show in figure 3 the calculated $g^{(2)}(0)$ as a function of $\Delta\omega_1$ and $\Delta\omega_2$, respectively. We truncate the Hilbert space to consider a maximum number of photons $N_{\rm max} = 12$ in the basis set of Fock states, which we checked to be sufficient for convergence. Realistic model parameters are assumed, as described in the previous section and reported in the figure caption. Again, we point out that all the energies are intended in units of $\hbar\gamma = 25\,\mu$eV, as explained above. The minimum value of $g^{(2)}(0)$ identifies the optimal operation detuning of the laser frequency from the bare resonators, which is $\Delta\omega_1 = \Delta\omega_2 \simeq 0.2$, for which $g^{(2)}(0) \simeq 0.42$.

While the previous parameter can be experimentally adjusted with a tunable laser as the input source, there are characteristics that depend on the specific device implementation. In particular, coupled modes of photonic crystal molecules may display asymmetric losses according to the mode parity, i.e. $\gamma_+ \neq \gamma_-$, as experimentally shown, e.g., in [46]. This effect is not surprising, since unbalanced Q-factors of symmetric and antisymmetric modes can be traced back to the peculiar loss mechanism in such planar photonic crystal cavities, where perturbative coupling to radiative modes depends on the mode parity with respect to a defined

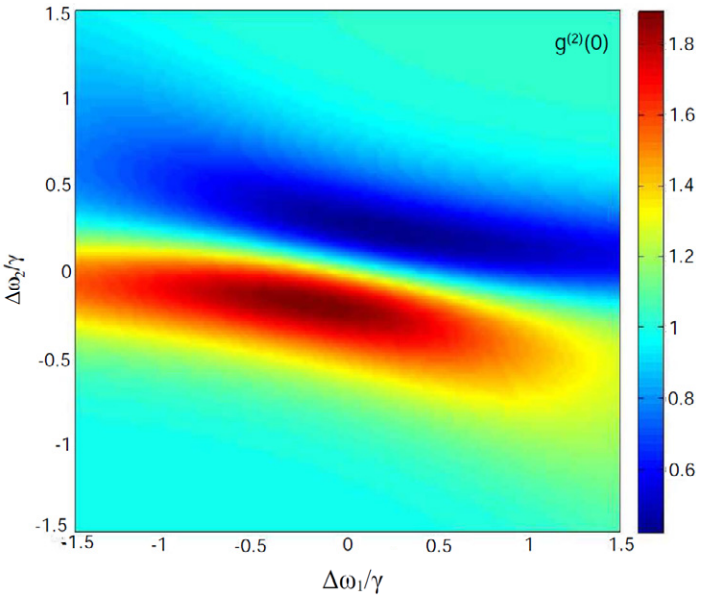

Figure 3. Numerical solution for the zero-time-delay second-order correlation represented in color scale plot as a function of $\Delta\omega_1 \neq \Delta\omega_2$, with parameters (units of $\hbar\gamma$): $\hbar\gamma = 25\,\mu$eV, $U_{\rm nl} = 4 \times 10^{-5}$ and $J = 56$, $F = 10$.

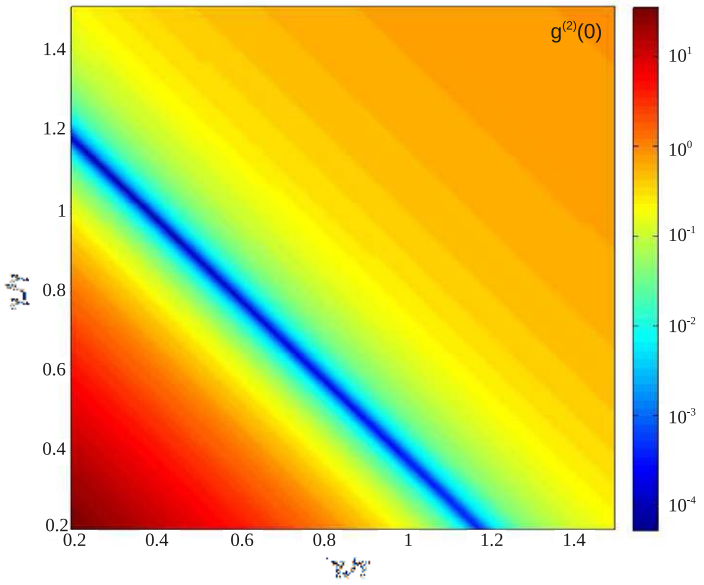

Figure 4. Color scale plot of the numerical solution for the zero-time-delay second-order correlation as a function of γ_+/γ and γ_-/γ, with parameters (in units of $\hbar\gamma = 25\,\mu$eV): $\Delta\omega_1 = \Delta\omega_2 = 0.2$, $F = 15$, $U_{\rm nl} = 4 \times 10^{-5}$ and $J = 56$.

symmetry plane of the system [48]. In figure 4, we consider the case in which the two resonators possess the same basic characteristics, i.e. the same frequency detunings $\Delta\omega_1 = \Delta\omega_2 = 0.2$, and the same dissipation rates for each isolated cavity mode, γ. We then study the behavior of the SPS in terms of the symmetric and antisymmetric modes losses. Numerical solutions are

reported for the zero-time-delay second-order correlation as a function of γ_+/γ and of γ_-/γ. Quite remarkably, the figure of merit is optimal for unbalanced losses, i.e. $\gamma_+ \neq \gamma_-$. In fact, breaking the symmetry of the system and for appropriate resonators parameters the photonic molecule in examination represents an almost ideal source of single-photon Fock states (down to $g^{(2)}(0) < 10^{-4}$). Incidentally, this is exactly the situation that is most naturally realized in a photonic crystal molecule [46], although not generally valid for any type of tunnel-coupled photonic resonators (such as, e.g., coupled microdiscs or micropillars).

The numerical results reported in figure 4 can be understood by employing a perturbative analytical treatment [31, 33]. The pump laser frequency in the present scheme is strongly off-resonance with respect to the two eigenfrequencies of the system, corresponding to the $\hat{a}_+$ and $\hat{a}_-$ modes, respectively. Hence, even under the conditions $F/(\hbar\gamma) \gg 1$, a low occupancy of the two modes is expected and the Hilbert space can be truncated to the two-photon occupancy in the basis of Fock states $\{|n_1, n_2\rangle\}$, with n_1 and n_2 counting the number of photons in the first and second mode, respectively. The mode losses can be treated at the Hamiltonian level by considering

$$\tilde{H} = \hat{H} - \mathrm{i}\frac{\hbar\gamma_+}{2}\hat{a}_+^\dagger\hat{a}_+ - \mathrm{i}\frac{\hbar\gamma_-}{2}\hat{a}_-^\dagger\hat{a}_-, \tag{9}$$

where $\hat{H}$ is given in equation (3). With a straightforward substitution, equation (9) can be written as

$$\tilde{H} = \sum_{i=1,2}[\tilde{\Delta}_i\hat{a}_i^\dagger\hat{a}_i + U_{\mathrm{nl}}\hat{a}_i^\dagger\hat{a}_i^\dagger\hat{a}_i\hat{a}_i] + \tilde{J}(\hat{a}_1^\dagger\hat{a}_2 + \hat{a}_2^\dagger\hat{a}_1) + F(\hat{a}_1^\dagger + \hat{a}_1), \tag{10}$$

where we have defined $\tilde{\Delta}_i = \hbar[\Delta\omega_i - (\gamma_+ + \gamma_-)/4]$ and $\tilde{J} = J - \hbar(\gamma_+ - \gamma_-)/4$. With the ansatz

$$|\psi\rangle = C_{00}|00\rangle + C_{10}|10\rangle + C_{01}|01\rangle + C_{20}|20\rangle + C_{11}|11\rangle + C_{02}|02\rangle + \ldots, \tag{11}$$

the steady-state solution can be found by solving the coupled equations for the coefficients $C_{n_1n_2}$ from $\mathrm{i}\hbar\frac{\partial}{\partial t}|\psi\rangle = \tilde{H}|\psi\rangle = 0$

$$\tilde{\Delta}C_{10} + JC_{01} + FC_{00} = 0, \tag{12}$$

$$\tilde{\Delta}C_{01} + JC_{10} = 0, \tag{13}$$

$$2(\tilde{\Delta} + U_{\mathrm{nl}})C_{20} + \sqrt{2}JC_{11} + \sqrt{2}FC_{10} = 0, \tag{14}$$

$$2\tilde{\Delta}C_{11} + \sqrt{2}J(C_{20} + C_{02}) + FC_{01} = 0, \tag{15}$$

$$2(\tilde{\Delta} + U_{\mathrm{nl}})C_{02} + \sqrt{2}JC_{11} = 0, \tag{16}$$

where we have approximated $\tilde{J} \simeq J$, since $J \gg \hbar\Delta\omega, U_{\mathrm{nl}}, \hbar\gamma$. Equations (12)–(16) can be simplified by considering the condition $C_{00} \simeq 1$ and $C_{00} \gg C_{10}, C_{01} \gg C_{20}, C_{11}, C_{02}$. The second-order correlation for light emitted from cavity 1 can be analytically approximated as $g^{(2)}(0) \simeq 2|C_{20}|^2/|C_{10}|^4$. Hence, minimizing $|C_{20}|^2$ with respect to $\Delta\omega_1 = \Delta\omega_2 = \Delta\omega$ (keeping fixed $\gamma_+ + \gamma_-$, J, U_{nl}), which corresponds to minimizing the complex function $|2\tilde{\Delta}^3 + J^2U_{\mathrm{nl}}|^2$, we obtain the optimal conditions for the antibunching behavior at a fixed $\Delta\omega$ as

$$[\gamma_+ + \gamma_-]_{\mathrm{opt}} \simeq 4\sqrt{3}\Delta\omega\,. \tag{17}$$

This result quantitatively explains the dependence of the optimal antibunching (minimum in $g^{(2)}(0)$) in figure 4. At small pumping rates, the value of $g^{(2)}(0)$ grows monotonically with

F [32]. In this sense, the smaller the pumping rate, the better the single photon behavior of the output. However, in a practical device this would also lead to a vanishingly small number of photons in the systems, and hence of single photons emitted from cavity 1. In our conditions, the average number of photons $\langle \hat{a}_1^\dagger \hat{a}_1 \rangle$ is always much smaller than 1, but of the order of 10^{-5}–10^{-4}, depending on the pumping strength, which means an expected single-photon emission rate of 10–100 kHz. In terms of SPS efficiency, the possibility of enhancing even further the single-photon emission rate (possibly beyond the MHz) is an unequivocal advantage of the present source as compared to typical heralded ones [7, 9].

A still open question, in view of actual applications of this scheme as an SPS, concerns the feasibility of pulsed operation, which would be required for single-photon emission on-demand. The delay dependence of $g^{(2)}(\tau)$ is determined by beatings between the two oscillators. It shows pronounced oscillations at a rate determined by the tunnel coupling, and the condition $g^{(2)}(\tau) < 1$ is fulfilled only over a delay of the order of $\tau \simeq \hbar/J$ [32, 33], i.e. much shorter than the photon lifetime. This feature prevents observation of photon antibunching in the pulsed excitation regime. However, it should be possible to address this issue by further processing the output of the two-cavity system. On the one hand, a post-selective temporal filter with a $\hbar/J$ delay window can be applied at the output of the coupled cavity device to ensure the presence of single-photon Fock states. Moreover, it was already shown that photon antibunching can be optimized in similar situations through passive interferometry [49] or active quantum feedback schemes [50]. In this sense, we believe that $g^{(2)}(0) \ll g^{(2)}(\tau)$ is a necessary condition to be optimized before realizing an SPS, but further analysis is needed to characterize its output, depending on the specific device implementation. Such an analysis is beyond the scope of the present work.

3.3. Effects of pure dephasing

In photonic crystal molecules, the loss mechanism naturally leads to unbalanced quality factors for the symmetric and antisymmetric modes with respect to the quality factor of the isolated cavity that can be of the order of $Q_-/Q_+ = \gamma_+/\gamma_- \sim 1 \to 10$. Neglecting the counterintuitive effect of possible antisymmetric ground states [47], the lower energy mode is usually the symmetric combination of the two isolated cavity states, which has a reduced quality factor as compared to the isolated cavity [46]. Thus, we extract from the color plot in figure 4 the curve corresponding to $\gamma_- = 0.2\gamma$ (i.e. the quality factor of the antisymmetric mode is larger than that of the isolated cavity). The curve is plotted in figure 5 (curve corresponding to $\gamma^* = 0$), showing a close-to-ideal antibunching of $g^{(2)}(0) \simeq 7 \times 10^{-5}$ for $\gamma_+ \simeq 1.2\gamma$, remarkably not far from the realistic ratio $\gamma_+/\gamma_- \simeq 3$ reported in the literature [46] for coupled photonic crystal cavities.

A possible source of unwanted loss channels that could potentially spoil the effects of photon blockade induced by tunnel coupling is pure dephasing. In a semiconductor cavity, dephasing can be due to thermal fluctuations or other nonlinear mechanisms enhanced by the same electromagnetic field confinement, giving rise to index fluctuations within the cavity region and hence a pure dephasing rate. Even if such an effect is usually neglected, and it is difficult to attribute a pure dephasing rate that is generally valid for any type of mechanism and material, it is of utmost importance to estimate such detrimental effects on the SPS figure of merit for the purposes of the present work. As discussed in section 2, the effects of pure dephasing can be simply modeled by solving the master equation after adding the Liouvillian

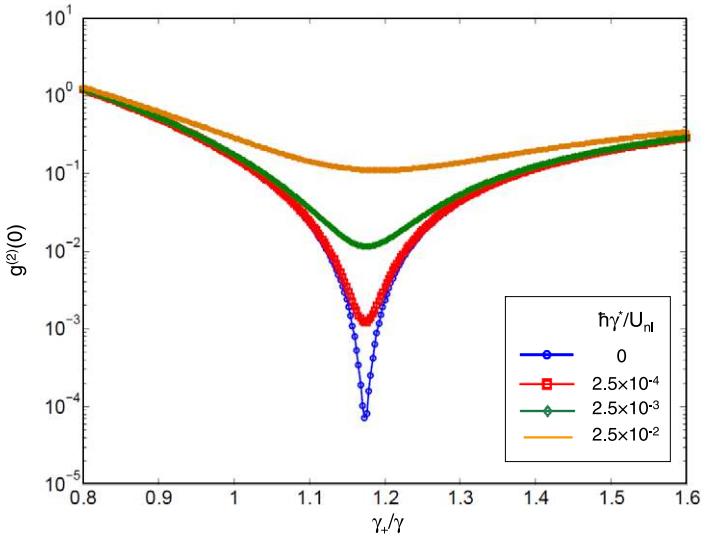

Figure 5. Numerical solution for the zero-time-delay second-order correlation as a function of γ_+/γ, for different values of pure dephasing rate (assumed equivalent for both symmetric and antisymmetric modes). Parameters are the same as in figure 4, with $\gamma_-/\gamma = 0.2$.

term of the form represented in equation (6). We report in figure 5 the calculated $g^{(2)}(0)$ as a function of γ_+/γ for $\gamma_-/\gamma = 0.2$ on increasing the pure dephasing rate, γ^*. Suppression of antibunching occurs for values of loss rates of the order of $\hbar\gamma^* \sim U_{\rm nl}$. Interestingly, the SPS figure of merit tolerance is such that at $\hbar\gamma^*/U_{\rm nl} \simeq 10^{-2}$ and $\gamma_+/\gamma \simeq 1.2$, the system still displays an acceptable single-photon nonlinear behavior with $g^{(2)}(0) \simeq 0.1$, which confirms the robustness of such a scheme even with respect to loss channels that are difficult to control in a real experimental setting. On the other hand, we expect that pure dephasing effects are most probably going to play a marginal role in the present scheme, where small pump powers are required to efficiently operate the SPS.

4. Conclusions

We have presented theoretical results supporting the proposal of a single-photon source built on an integrated photonic platform made of passive material components, where cavity-enhanced native nonlinearities are able to produce single-photon blockade. The building block is based on tunnel-coupled resonators, or photonic molecules, coherently driven by an external laser source. We have provided numerical evidence for the best combination of system parameters, such as cavity-laser detunings and modes losses, leading to optimal antibunching of the output signal. In particular, we found that a close to ideal single-photon output can be obtained from asymmetric losses of the coupled modes, as it naturally occurs in photonic crystal molecules. The robustness of such a device is tested against unwanted loss channels, e.g. giving rise to pure dephasing of the normal modes.

Further analysis will be needed to engineer the output of the device as a useful single-photon wave packet for actual applications in integrated quantum circuits. However, the results

presented here provide a useful starting point to design highly innovative quantum photonic devices based on integrated sources of pure single-photon states. The main innovations come from the possibility of employing commonly nano-structured materials from the optoelectronic and CMOS-compatible industry, working at room temperature, and in the telecom band for long-distance low-loss data transmission. We believe that this work will further stimulate research in this direction, also in view of recent experimental demonstrations of enhanced native optical nonlinearities in semiconductor-based photonic crystal platforms [43–45].

Acknowledgments

We acknowledge Timothy C H Liew for contributing to the early stages of these calculations and for useful comments and suggestions and L C Andreani, D Bajoni, I Carusotto, M Galli, L O'Faolain and T F Krauss for stimulating discussions concerning the physics and the realization of this proposal. This work was partly supported by the NanoSci-ERANET project 'LECSIN'. S Ferretti acknowledges support from Fondazione Cariplo under project 2010-0523.

References

[1] O'Brien J L, Furusawa A and Vučković J 2009 *Nature Photon.* **3** 687
[2] O'Brien J L, Patton B, Sasaki M and Vučković J (ed) 2011 Focus on integrated quantum optics *New J. Phys.* 14 (special issue)
[3] Knill E *et al* 2001 *Nature* **409** 46
[4] Kiraz A, Atatüre M and Imamoğlu A 2004 *Phys. Rev.* A **69** 032305
[5] Politi A, Cryan M J, Rarity J G, Yu S Y and O'Brien J L 2008 *Science* **320** 646
Politi A, Matthews J C F and O'Brien J L 2009 *Science* **325** 1221
[6] Hong C K and Mandel L 1986 *Phys. Rev. Lett.* **56** 58
Pittman T B, Jacobs B C and Franson J D 2002 *Phys. Rev.* A **66** 042303
[7] Fasel S, Alibart O, Tanzilli S, Baldi P, Beveratos A, Gisin N and Zbinden H 2004 *New J. Phys.* **6** 163
[8] Grangier P, Sanders B and Vučković J (ed) 2004 Focus on single photons on demand *New J. Phys.* 6 (special issue)
[9] Davanço M *et al* 2012 *Appl. Phys. Lett.* **100** 261104
[10] Loudon R 1983 *The Quantum Theory of Light* (Oxford: Oxford University Press)
[11] Kuhn A and Ljunggren D 2010 *Contemp. Phys.* **51** 289–313
[12] Tian L and Carmichael H J 1992 *Phys. Rev.* A **46** 6801
[13] Werner M J and Imamoğlu A 1999 *Phys. Rev.* A **61** 011801
[14] Michler P, Kiraz A, Becher C, Schoenfeld W V, Petroff P M, Zhang L, Hu E and Imamoğlu A 2000 *Science* **290** 2282
[15] Pelton M, Santori C, Vučković J, Zhang B, Solomon G S, Plant J and Yamamoto Y 2002 *Phys. Rev. Lett.* **89** 233602
[16] Santori C, Fattal D, Vučković J, Solomon G S and Yamamoto Y 2002 *Nature* **419** 594
[17] Hennessy K, Badolato A, Winger M, Gerace D, Atatüre M, Gulde S, Fält S, Hu E L and Imamoğlu A 2007 *Nature* **445** 896
[18] Press D, Götzinger S, Reitzenstein S, Hofman C, Löffler A, Kamp M, Forchel A and Yamamoto Y 2007 *Phys. Rev. Lett.* **98** 117402
[19] Claudon J, Bleuse J, Malik N S, Bazin M, Jaffrennou P, Gregersen N, Sauvan C, Lalanne P and Gérard J-M 2010 *Nature Photon.* **4** 174
[20] Manga Rao V S C and Hughes S 2007 *Phys. Rev. Lett.* **99** 193901

[21] Schwagmann A, Kalliakis S, Farrer I, Griffiths J P, Jones G A C, Ritchie D A and Shields A J 2011 *Appl. Phys. Lett.* **99** 261108
[22] Laucht A *et al* 2012 *Phys. Rev.* X **2** 011014
[23] Faraon A, Fushman I, Englund D, Stoltz N, Petroff P and Vučković J 2008 *Nature Phys.* **4** 859
[24] Reinhard A, Volz T, Winger M, Badolato A, Hennessy K J, Hu E L and Imamoğlu A 2012 *Nature Photon.* **6** 93
[25] Imamoğlu A, Schmidt H, Woods G and Deutsch M 1997 *Phys. Rev. Lett.* **79** 1467
[26] Birnbaum K M, Boca A, Miller R, Boozer A D, Northup T E and Kimble H J 2005 *Nature* **436** 87
[27] Rebić S, Parkins A S and Tan S M 2004 *Phys. Rev.* A **69** 035804
[28] Verger A, Ciuti C and Carusotto I 2006 *Phys. Rev.* B **73** 193306
[29] Gerace D, Türeci H E, Imamoğlu A, Giovannetti V and Fazio R 2009 *Nature Phys.* **5** 281
[30] Carusotto I, Volz T and Imamoğlu A 2010 *Europhys. Lett.* **90** 37001
[31] Ferretti S, Andreani L C, Türeci H E and Gerace D 2010 *Phys. Rev.* A **82** 013841
[32] Liew T C H and Savona V 2010 *Phys. Rev. Lett.* **104** 183601
[33] Bamba M, Imamoğlu A, Carusotto I and Ciuti C 2011 *Phys. Rev.* A **83** 021802
[34] Boyd R W 2008 *Nonlinear Optics* (New York: Academic)
[35] Ferretti S and Gerace D 2012 *Phys. Rev.* B **85** 033303
[36] Kuramochi E, Notomi M, Mitsugi S, Shinya A, Tanabe T and Watanabe T 2006 *Appl. Phys. Lett.* **88** 041112
Asano T, Song B-S and Noda S 2006 *Opt. Express* **14** 1996
[37] Nakayama S, Ishida S, Iwamoto S and Arakawa Y 2011 *Appl. Phys. Lett.* **98** 171102
[38] Carmichael H J 1985 *Phys. Rev. Lett.* **55** 2790
[39] Liew T C H and Savona V 2012 *Phys. Rev.* A **85** 050301
[40] Drummond P D and Walls D F 1980 *J. Phys. A: Math. Gen.* **13** 725
[41] Vahala K J 2003 *Nature* **424** 839
[42] Notomi M 2010 *Rep. Prog. Phys.* **73** 096501
[43] Combrié S, De Rossi A, Tran N-Q-V and Benisty H 2008 *Opt. Lett.* **33** 1908
[44] Galli M, Gerace D, Welna K, Krauss T F, O'Faolain L, Guizzetti G and Andreani L C 2010 *Opt. Express* **18** 26613
[45] Gu T, Petrone N, McMillan J F, van der Zande A, Yu M, Lo G Q, Kwong D L, Hone J and Wong C W 2012 *Nature Photon.* **6** 554
[46] Atlasov K A, Karlsson K F, Rudra A, Dwir B and Kapon E 2008 *Opt. Express* **16** 16255
[47] Caselli N *et al* 2012 *Phys. Rev.* B **86** 035133
[48] Andreani L C and Gerace D 2006 *Phys. Rev.* B **73** 235114
[49] Qu Y, Xiao M, Holliday G S, Singh S and Kimble H J 1992 *Phys. Rev.* A **45** 4932
[50] Smith W P, Reiner J E, Orozco L A, Kuhr S and Wiseman H M 2002 *Phys. Rev. Lett.* **89** 133601